Amorphous Phase of Propylene/Ethylene Copolymers Characterized by Positron Annihilation Lifetime Spectroscopy

H. P. Wang,[†] P. Ansems,[‡] S. P. Chum,[‡] A. Hiltner,*[,†] and E. Baer[†]

Department of Macromolecular Science, and Center for Applied Polymer Research, Case Western Reserve University, Cleveland, Ohio 44106-7202, and Polyolefins and Elastomers R & D, The Dow Chemical Company, Freeport, Texas 77541

Received October 4, 2005; Revised Manuscript Received November 23, 2005

ABSTRACT: Recent advances in catalyst technology make it possible to synthesize high molecular weight propylene copolymers with a high degree of isotacticity and high levels of an α-olefin comonomer. The primary objective of this study is to systematically characterize the rubbery amorphous phase of propylene/ethylene (P/E) copolymers over a range in comonomer content. A series of new experimental P/E copolymers prepared with a group IV transition metal-based post-metallocene catalyst are compared with a series of P/E copolymers prepared with a conventional metallocene catalyst. Positron annihilation lifetime spectroscopy (PALS) is used to obtain the temperature dependence of the free volume hole size. The PALS measurements are supplemented with bulk volume−temperature measurements. It is found that the free volume hole size and the amorphous phase density at ambient temperature strongly depend on crystallinity. Densification of the amorphous phase is attributed to constraint imposed on rubbery amorphous chain segments by attached chain segments in crystals. It is now possible to attribute the reported discrepancy between conventional measurements of crystallinity from density and crystallinity from heat of melting to the crystallinity dependence of the amorphous phase density. The fractional free volume (*FFV*) of the amorphous phase is obtained by combining the free volume hole size with the macroscopic volume−temperature measurement. At the glass transition temperature the *FFV* is constant across the crystallinity range of the P/E copolymers with a value of about 0.04, in agreement with iso-free volume concepts of the glass transition.

Introduction

Recent advances in catalyst technology have made it possible to synthesize high molecular weight propylene copolymers with relatively high levels of an α-olefin comonomer. Of particular interest are the propylene/ethylene copolymers produced by The Dow Chemical Co. using a recently developed group IV transition metal-based post-metallocene catalyst.[1] These copolymers exhibit high molecular weight, relatively narrow molecular weight distribution, and unique chain microstructures. Unlike metallocene-catalyzed copolymers, which have homogeneous comonomer distribution, the new copolymers are characterized by heterogeneous chain composition and different defect distribution.[2]

Like ethylene/α-olefin copolymers,[3,4] the new propylene/ethylene copolymers exhibit a wide spectrum of solid-state structures and properties.[5] The crystalline morphology ranges from space-filling spherulites at low comonomer content to non-space-filling embryonic axialites in copolymers with high ethylene content. As a consequence, the mechanical properties range from typical thermoplastic behavior to elastomeric behavior.

Our previous structure−property studies of propylene copolymers focused primarily on the crystalline phase.[5−7] However, isotactic propylene homopolymers are ∼50% noncrystalline, and the amorphous fraction increases with the comonomer content. Compared with the highly ordered crystalline phase, insight into the amorphous phase, and its relationship to the crystalline phase, is particularly elusive. Even in conventional propylene homopolymers, the nature of the amorphous phase is not entirely understood as evidenced by unresolved differences in the degree of crystallinity measured by different techniques.[8]

It is well accepted that the amorphous phase contains excess free volume as a result of less efficient chain packing compared with the crystalline phase.[9] The type and amount of free volume affect chain dynamics and impact mechanical properties and diffusion phenomena. One of the most powerful molecular-scale probes of the amorphous phase free volume is positron annihilation lifetime spectroscopy (PALS).[10−12] Briefly, the positronium (Ps) particle, which forms by combination of a thermal positron with an electron in the host polymer, is preferentially localized in the free volume holes. The primary annihilation mechanism of the triplet Ps species (orthopositronium, o-Ps) is with electrons of the host polymer. The lifetime of o-PS is particularly sensitive to the size of the free volume hole in which it is located. Thus, the average free volume hole size can be quantitatively extracted from the o-Ps annihilation lifetime component of PALS. The combination of PALS with the macroscopic volume−temperature measurement allows the number of holes and the fractional free volume (*FFV*) to be estimated.[13−15]

The primary objective of this study is to systematically examine the amorphous phase of propylene/ethylene copolymers. We compare a series of new experimental P/E copolymers with a series of metallocene-catalyzed P/E copolymers. By increasing the ethylene content, the crystallinity of the copolymer is reduced to less than 10 wt %. Volume−temperature measurements are used in combination with PALS to support our understanding.

Materials and Methods

Polypropylene and propylene/ethylene copolymers, prepared by an experimental group IV post-metallocene catalyst (xP/E) and by

* Corresponding author. E-mail: ahiltner@case.edu.
[†] Case Western Reserve University.
[‡] The Dow Chemical Company.

10.1021/ma0521506 CCC: $33.50
Published on Web 01/21/2006

a conventional metallocene catalyst (mP/E), were supplied in pellet form by The Dow Chemical Co., together with information on comonomer content, molecular weight, and molecular weight distribution as given in Table 1. The polymers are designated by the type of catalyst and the ethylene content in mole percent.

Films were compression-molded from the pellets at 190 °C and cooled to ambient temperature at ~15 °C min^{-1} in the press. The compression-molded films were subsequently aged 7−12 days at ambient temperature before measuring the physical properties. Thermal analysis was performed on a Perkin-Elmer DSC-7 from −60 to 190 °C with a heating/cooling rate of 10 °C min^{-1}. Weight percent crystallinity was calculated from

$$X_{c,\Delta H}(\text{wt \%}) = \frac{\Delta H_m}{\Delta H_m^\circ} \times 100\% \quad (1)$$

where ΔH_m is the measured specific heat of melting and ΔH_m° is the heat of fusion of the polypropylene crystal taken to be 209 J g^{-1}.[16,17]

The glass transition temperature (T_g) was determined by dynamic mechanical thermal analysis (DMTA) of aged P/E films using a Polymer Laboratories dynamic mechanical thermal analyzer. Specimens were tested in dynamic tension with 1% strain at 1 Hz from −80 to 10 °C below the melting temperature at a scanning rate of 3 °C min^{-1}.

The density was measured according to ASTM D1505-85. A 2-propanol/water gradient column with a range of 0.8−1.0 g cm^{-3} was used. Small pieces of film (~2 × 2 mm^2) were placed in the column and allowed to equilibrate for 1 h before measurement. To measure density in the temperature range from −15 to 25 °C, a circulating ethanol bath was connected to the jacket of the density column. Density measurements were taken 1 h after the column temperature had stabilized. The reported density is the average of at least three specimens and has an error of less than 0.0005 g cm^{-3}. Measurements at low temperatures were limited by icing of the 2-propanol/water solution inside the gradient column.

Positron annihilation lifetime spectroscopy (PALS) was performed using the fast−fast coincident method with a time resolution of 230 ps, at a count rate of ~10^6 counts/h.[15,18] A 30 μCi ^{22}NaCl positron source was sandwiched in between two compression-molded films, each with thickness of 1 mm and 1 × 1 cm^2 area. Temperature measurements were taken by first decreasing the temperature as low as −100 °C and then allowing 1 h for equilibrium before the temperature was sequentially increased in steps of 5 or 10 °C. At each temperature, a spectrum containing a total of 10^6 counts was collected over 1 h after allowing 20 min for temperature equilibrium. In addition, one of the copolymers (xP/E12.1) was left in the positron source for 48 h at 23 °C to test for possible effects of prolonged exposure. However, no change in the PALS spectrum was observed.

The positron lifetime spectrum was determined by PATFIT software. The spectra were fitted to three exponentially decaying lifetime components. The average free volume hole radius (r_h) was calculated from the o-Ps lifetime (τ_3) using the semiempirical equation[10,11]

$$\tau_3(\text{ns}) = 0.5\left[1 - \frac{r_h}{r_h + \delta r} + \frac{1}{2\pi}\sin\left(\frac{2\pi r_h}{r_h + \delta r}\right)\right]^{-1} \quad (2)$$

where δr has been empirically determined to be $\delta r = 0.1656$ nm by fitting eq 2 to the o-Ps annihilation data for molecular solids of known pore size.[11] The uncertainty in r_h based on 10 spectra was ±0.02 Å. The free volume hole size, (v_h) was calculated as $v_h = 4\pi r_h^3/3$ assuming spherical holes.

Results

Crystallinity. The effects of comonomer content on the physical properties of the mP/Es and the xP/Es used in this study are described in detail elsewhere.[5] The results for the density (ρ), the melting temperature (T_m), the heat of melting (ΔH_m), and the glass transition temperature (T_g) are summarized in Table 2. As shown in Figure 1, for both mP/Es and xP/Es, crystallinity as reflected by ΔH_m decreased linearly with increasing comonomer content. However, the crystallinity of xP/Es was consistently lower than the crystallinity of mP/Es for a given comonomer content. Both xP/Es and mP/Es possess a high degree of isotacticity in the propylene sequences. The difference in crystallinity was attributed primarily to differences in comonomer distribution and defect type. It is reported that the distribution of ethylene units in mP/Es is close to statistical, whereas the distribution in xP/Es is more alternating.[2] This means that, for a given comonomer content, xP/Es have shorter propylene blocks than mP/Es, resulting in less crystallizable xP/E chains. The regio-defect concentration in xP/Es is about 0.4 mol %,[2] which is comparable to the reported regio-defect concentration in metallocene-catalyzed propylene/ethylene copolymers.[19] However, xP/Es show a unique regio-defect.[2] In mP/Es a regio-defect tends to be followed by a propylene unit, but in xP/Es by an ethylene unit. The regio-defect of xP/E might be more effective in disrupting crystallization.

Table 1. Characteristics of Propylene/Ethylene Polymers

polymer designation	comonomer content (mol %)	M_w (kg mol^{-1})	M_w/M_n
xP/E0.0	0.0	316	2.7
xP/E4.3	4.3	329	2.2
xP/E7.6	7.6	296	2.2
xP/E12.1	12.1	285	3.1
xP/E16.1	16.1	262	2.2
xP/E19.2	19.2	263	2.4
mP/E0.0	0.0	282	2.2
mP/E3.1	3.1	318	2.0
mP/E11.0	11.0	150	2.3
mP/E13.6	13.6	110	2.1
mP/E18.8	18.8	201	2.1
mP/E25.2	25.2	219	2.1

The weight fraction crystallinity $X_{c,\Delta H}$ from DSC, taking ΔH_m° of 209 J g^{-1},[16,17] was compared with weight fraction crystallinity from density, $X_{c,\rho}$, assuming a two-phase model with constant amorphous phase and crystalline phase densities

$$X_{c,\rho}(\text{wt \%}) = \frac{\rho_c}{\rho}\left(\frac{\rho - \rho_a}{\rho_c - \rho_a}\right) \times 100\% \quad (3)$$

where ρ, ρ_a, and ρ_c are the bulk density, amorphous phase density, and crystalline phase density, respectively. Using the generally accepted values of ρ_a and ρ_c for polypropylene of 0.853 g cm^{-3} and 0.936 g cm^{-3}, respectively,[20] crystallinity from density was consistently higher than crystallinity from DSC heat of melting (Figure 2). Using a somewhat higher value of 0.946 g cm^{-3} for ρ_c[8] reduced the discrepancy somewhat; nevertheless, the difference between the crystallinity calculations remained significant. Alternatively, the constant value taken for ρ_a in eq 3 may not be appropriate. The assumed value of 0.853 g cm^{-3} is taken from amorphous, atactic polypropylene, and it may not be appropriate if crystalline constraint affects chain packing in the amorphous phase.

Glass Transition. The dynamic mechanical relaxation behavior of xP/Es is shown in Figure 3 in the form of storage modulus (E'), loss modulus (E''), and loss tangent (tan δ). The effect of comonomer content and the comparison between mP/Es and xP/Es were consistent with previous observations.[5] It can be seen from Figure 3b,c that both E'' and tan δ showed a local maximum in the range of −25 to 15 °C that is identified conventionally as the β-relaxation. The glass transition temperature (T_g) of the amorphous phase was taken as the peak temperature of the β-relaxation. In both E'' and tan δ, the

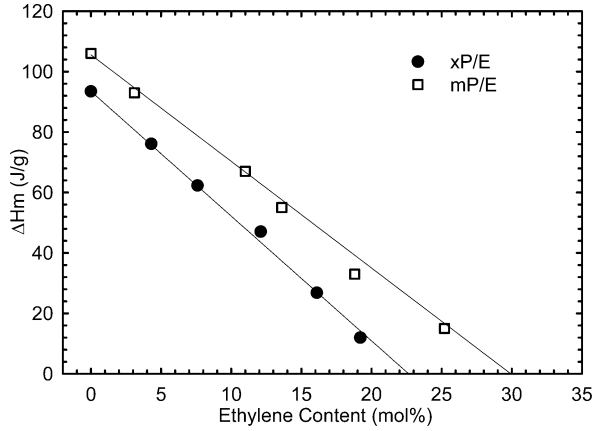

Figure 1. Effect of ethylene content as mol % on the heat of melting of P/E copolymers. ΔH_m was obtained from the first heating DSC thermogram.

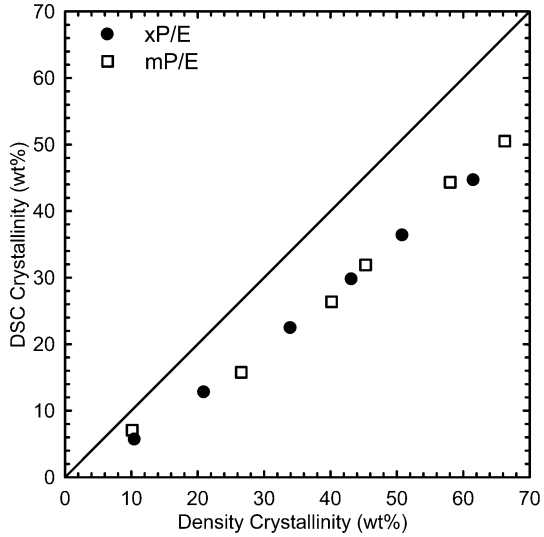

Figure 2. Comparison of crystallinity from density and crystallinity from DSC heat of melting.

β-relaxation peak shifted to higher temperature with increasing crystallinity. The T_g from the tan δ curves is tabulated as $T_{g,DMTA}$ in Table 2. The E'' peak temperature ($T_{g,E''}$), which may be a more appropriate measure of T_g than the tan δ peak temperature,[21] was consistently about 5 °C lower. For comparison, T_g from the inflection in the DSC thermogram is also included as $T_{g,DSC}$.

Amorphous Density. Figure 4 shows the specific volume ($v = 1/\rho$) of P/E copolymers as a function of temperature in the temperature range between −15 and 25 °C. Good reversibility was achieved in the density measurement between heating and cooling cycles in the gradient column in this temperature range. Therefore, only the results from the heating cycle are shown. For each polymer, linear thermal expansion was observed above T_g, where the amorphous phase was in the rubbery state. A linear region below T_g was not obtained due to the broad glass transition and icing of the 2-propanol/water solution inside the gradient column. The bulk thermal expansivity, defined as the slope $e_r = dv/dT$ (Table 2), decreased significantly with increasing crystallinity as a result of the significant difference in thermal expansivity of the crystalline and amorphous phases. However, the values were generally within the range that has been reported for polypropylene, i.e., from 5.5×10^{-4} to 9.4×10^{-4} cm^3 g^{-1} K^{-1}.[22]

The specific volume of the amorphous phase ($v_a = 1/\rho_a$) was calculated using crystallinity from DSC according to

$$v_a(T) = \frac{v(T) - v_c(T)X_{c,\Delta H}}{1 - X_{c,\Delta H}} \tag{4}$$

and the results are plotted in Figure 5. To obtain $v_c(T)$, values of the polypropylene crystal specific volume $v_c(23\ °C) = 1.068$ cm^3 g^{-1} ($\rho_c = 0.936$ g cm^{-3})[22] and thermal expansivity $e_c = 1.0 \times 10^{-4}$ cm^3 g^{-1} K^{-1} were obtained by fitting low-temperature data from ref 23. It is also assumed that the crystallinity did not change in this temperature range. The thermal expansivity of the rubbery amorphous phase, $e_{r,a} = dv_a/dT$, was obtained by linearly fitting the $v_a - T$ data above T_g for all P/Es, and the results are listed in Table 2. For $T > T_g$, the material with higher crystallinity always had lower amorphous phase specific volume (higher density) and lower thermal expansivity. The thermal expansivity of the amorphous phase decreased significantly with increasing crystallinity from 8.6×10^{-4} cm^3 g^{-1} K^{-1} for xP/E19.2 ($X_c = 6\%$) to 6.6×10^{-4} cm^3 g^{-1} K^{-1} for xP/E0.0 ($X_c = 45\%$). Similar results were found for the mP/E copolymers. It follows that decreasing bulk thermal expansivity as seen in Figure 4 cannot be attributed only to increasing crystallinity but includes the effect of decreasing amorphous phase thermal expansivity.

The amorphous density at 23 °C calculated from eq 4 is plotted in Figure 6 as a function of the crystallinity. The amorphous density of P/E copolymers increased with increasing crystallinity from 0.857 g cm^{-3} for xP/E19.2 ($X_c = 6\%$) to 0.877 g cm^{-3} for xP/E0.0 ($X_c = 45\%$). A similar trend was observed for mP/Es. A linear extrapolation to $X_c = 0$ gave $\rho_a = 0.854$ g cm^{-3} for the density of completely amorphous polypropylene, which coincided with the value measured for amorphous atactic polypropylene. The increase in ρ_a and the decrease in $e_{r,a}$ with increasing crystallinity were attributed to constraint on amor-

Table 2. Properties of Propylene/Ethylene Polymers

polymer	density (g cm^{-3})	$X_{c,\rho}$[a] (wt %)	T_m (°C)	ΔH_m (J g^{-1})	$X_{c,\Delta H}$[b] (wt %)	$T_{g,DSC}$ (°C)	$T_{g,DMTA}$[c] (°C)	$T_{g,E''}$ (°C)	ρ_a[d] (g/cm^{-3})	$e_r \times 10^4$ (cm^3 g^{-1} K^{-1})	$e_{r,a} \times 10^4$ (cm^3 g^{-1} K^{-1})
xP/E0.0	0.9022	61	145	93	45	N/A	12	10	0.877	4.0	6.6
xP/E4.3	0.8932	51	121	76	36	−11	7	0	0.870	5.1	7.2
xP/E7.6	0.8869	43	98	62	30	−17	0	−5	0.868	5.6	7.6
xP/E12.1	0.8795	34	84	47	22	−23	−6	−12	0.864	6.1	8.2
xP/E16.1	0.8691	21	44	27	13	−25	−14	−18	0.860	7.8	8.5
xP/E19.2	0.8610	10	44	12	6	−31	−20	−23	0.857	8.2	8.6
mP/E0.0	0.9062	66	152	106	51	N/A	10		0.878	3.6	6.2
mP/E3.1	0.8993	58	135	93	44	−12	5		0.872	4.3	7.0
mP/E11.0	0.8887	45	103	67	32	−19	−2		0.868	5.3	7.4
mP/E13.6	0.8845	40	92	55	26	−22	−6		0.867	5.7	7.5
mP/E18.8	0.8736	27	71	33	16	−27	−15		0.863	7.1	8.2
mP/E25.2	0.8607	10	56	15	7	−33	−17		0.855	8.2	8.8

[a] Crystallinity from density. [b] Crystallinity from heat of melting. [c] From tan δ. [d] At 23 °C.

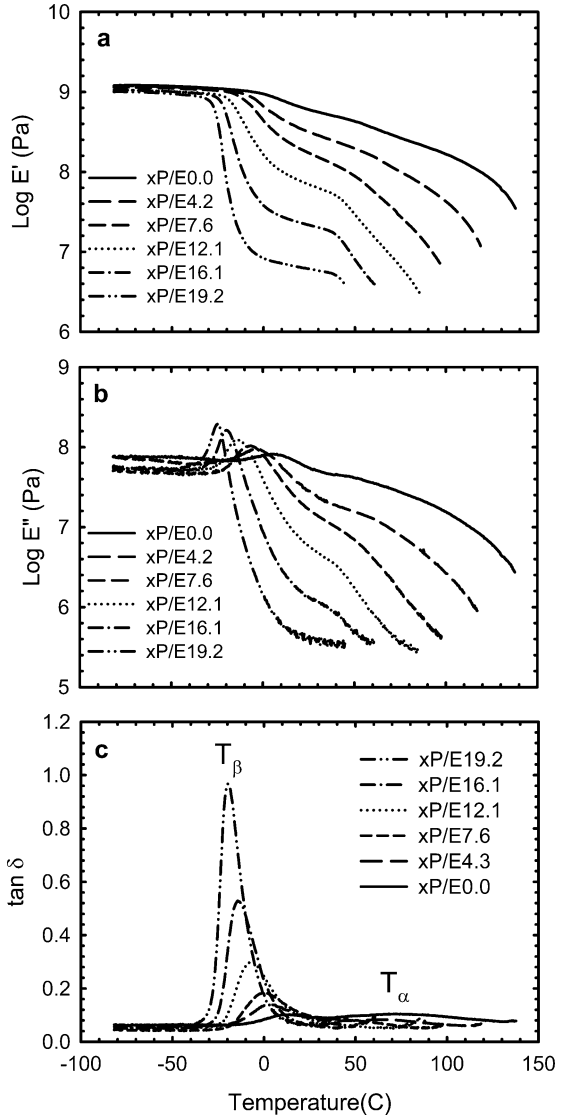

Figure 3. Dynamic mechanical relaxation behavior of xP/E copolymers: (a) log E'; (b) log E''; and (c) tan δ.

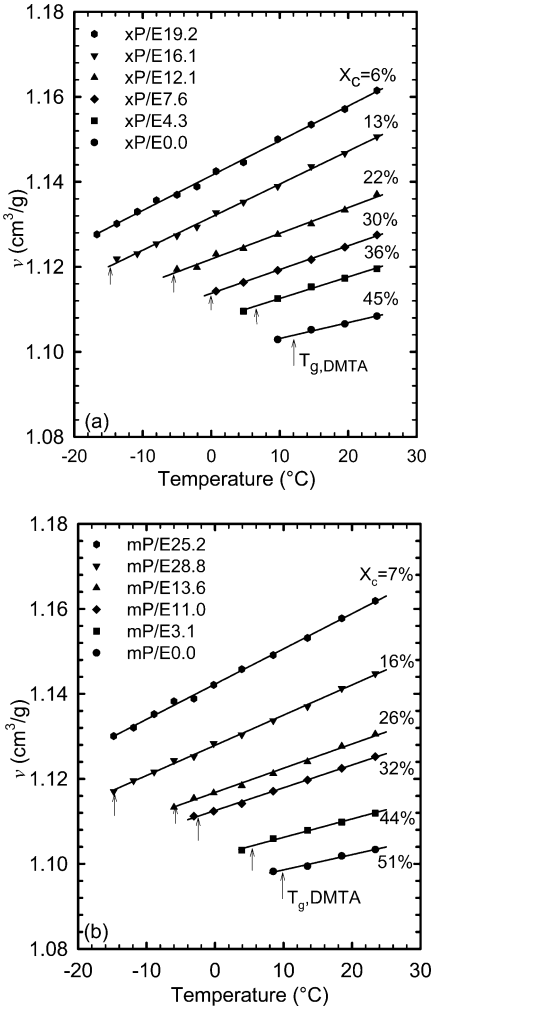

Figure 4. Temperature dependence of the specific volume, v: (a) xP/E series and (b) mP/Es series. The solid lines are the linear least-square fit above $T_{g,DMTA}$, as indicated by the arrows.

phous chains imposed by attachment to chain segments in crystals. Linear extrapolation of amorphous phase density to $X_c = 100$ gave a hypothetical value of $\rho_a = 0.900$ g cm^{-3} for completely constrained amorphous chain segments.

Free Volume Hole Size and Fraction. The free volume hole size (v_h) is plotted in Figure 7 as a function of temperature. For clarity, the data are shifted vertically by 30 Å^3. For xP/E0.0, the hole size varied from $v_h = 72$ Å^3 ($r_h = 2.58$ Å) at −70 °C to $v_h = 164$ Å^3 ($r_h = 3.40$ Å) at 70 °C with a distinct increase in the slope of the temperature dependence around 10 °C. The data were fitted by two straight lines with different slopes, and $T_{g,PALS}$ was obtained at the intersection. Values of $T_{g,PALS}$, which are listed in Table 3, correspond most closely to $T_{g,DMTA}$ for both xP/Es and mP/Es.

Below $T_{g,PALS}$, the hole thermal expansivity ($e_{h,g}$) obtained from the slope of the v_h-T curves was essentially constant with $e_{h,g} = 0.20$ Å^3 K^{-1} for all the xP/Es and $e_{h,g} = 0.25$ Å^3 K^{-1} for all the mP/Es (Table 3). However, above $T_{g,PALS}$ in the rubbery state, the hole thermal expansivity ($e_{h,r}$) decreased with increasing crystallinity, for example from 1.49 Å^3 K^{-1} for xP/E19.2 to 1.27 Å^3 K^{-1} for xP/E0.0. In the glassy state where the motion of chain segments is frozen, v_h represents the average size of static holes.[24,25] The small increase of v_h with temperature ($e_{h,g} \sim 0.20$ Å^3 K^{-1}) reflects the thermal expansion of free volume in the glassy state. When the amorphous phase is in the rubbery state, v_h is the average value of holes whose size and shape fluctuate in space and time.[24,25] The chain mobility results in a significant increase in the hole size with temperature.

The effect of crystallinity on free volume hole size is examined by comparing the free volume hole size of xP/E copolymers in the rubbery state (23 °C), at the glass transition temperature (T_g), and in the glassy state (−70 °C) (Figure 8). At ambient temperature (23 °C) v_h decreased significantly with increasing crystallinity, from about 140 Å^3 for xP/E19.2 to about 100 Å^3 for xP/E0.0. At T_g, there was a slight increase in v_h with crystallinity. Well below T_g, at −70 °C, v_h was essentially independent of crystallinity.

It is also of interest to estimate the number of free-volume holes in the amorphous phase. The number density of free volume holes can be determined from the relationship[13,15]

$$v_a = v_{occ} + N_h' v_h \tag{5}$$

where v_a is the specific volume of amorphous phase, v_{occ} is the occupied specific volume, N_h' is the number of holes per mass unit in the amorphous phase, and v_h is the average hole size. By assuming v_{occ} and N_h' are independent of temperature, N_h' can be determined from the linear fit of v_a-v_h plots.[15,26,27] Only results for $T > T_g$ are plotted in Figure 9. In all cases, good linear fits were obtained, and for clarity, only the data and fits

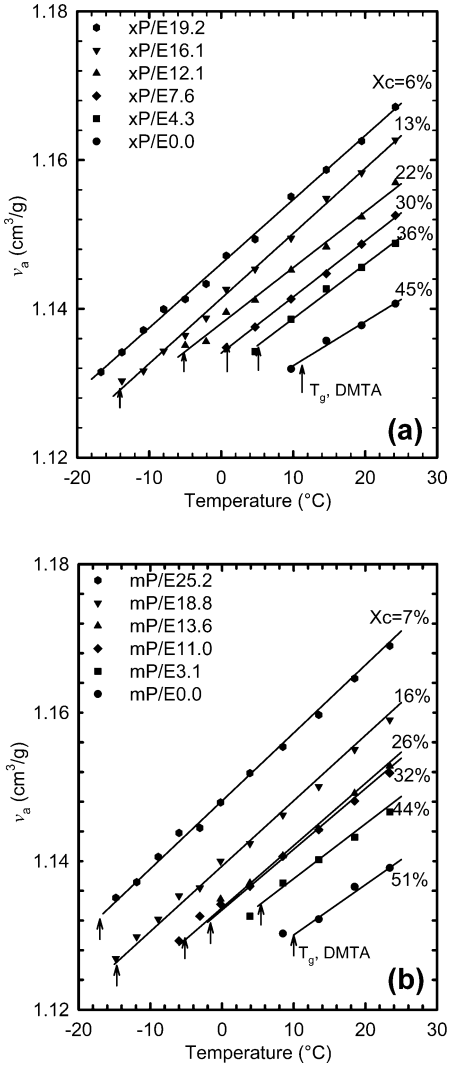

Figure 5. Temperature dependence of the amorphous phase specific volume, v_a: (a) xP/E series and (b) mP/E series. The solid lines are the linear least-square fit above $T_{g,DMTA}$, as indicated by the arrow.

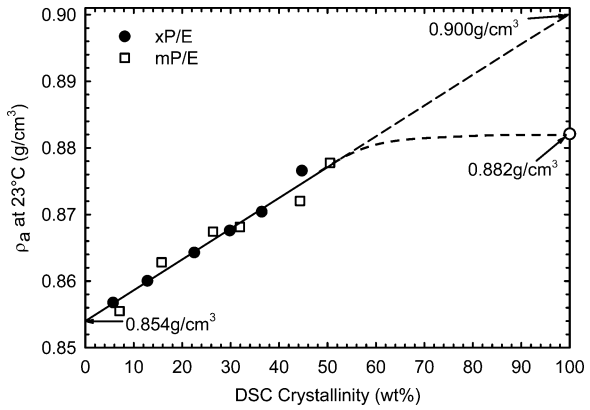

Figure 6. Amorphous phase density at 23 °C from eq 4 as a function of crystallinity from DSC heat of melting.

for xP/E0.0, xP/E7.6, mP/E0.0, and mP/E3.1 are shown as examples. The number of holes per mass unit in the amorphous phase (N_h') is tabulated in Table 3, together with the hole density at 23 °C (N_h) and v_{occ}. The value of N_h' for the amorphous phase for various P/E copolymers falls in the range $(5.1-5.9) \times 10^{20}$ g^{-1}, which is in agreement with reported values for isotactic propylene/α-olefin copolymers.[14]

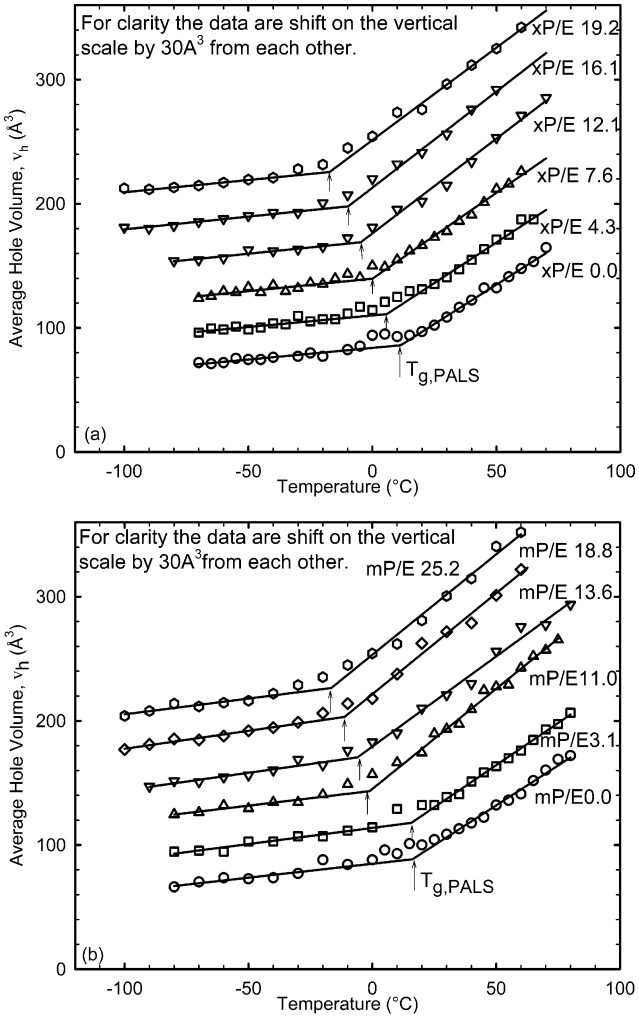

Figure 7. Temperature dependence of the average free-volume hole size, v_h: (a) xP/E series and (b) mP/E series. For clarity, the data are shifted on the vertical scale by 30 Å. The solid lines are the linear least-square fit below and above $T_{g,PALS}$, as indicated by the arrows.

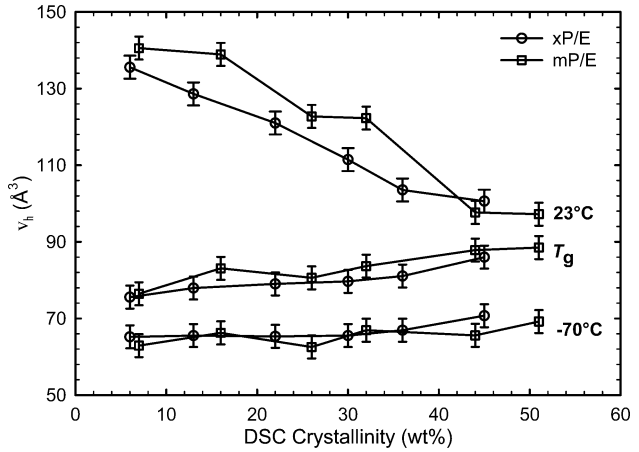

Figure 8. Effect of crystallinity on the average free volume hole size at three representative temperatures: 23 °C, T_g, and −70 °C.

Discussion

It is now possible to construct the temperature dependence of the amorphous phase specific volume (v_a-T). As a noncrystallizable polymer is cooled from the melt, it contracts along an equilibrium liquid line until it intersects the nonequilibrium glassy expansion line at the glass transition temperature (Figure 10). The equilibrium liquid line is established with data from

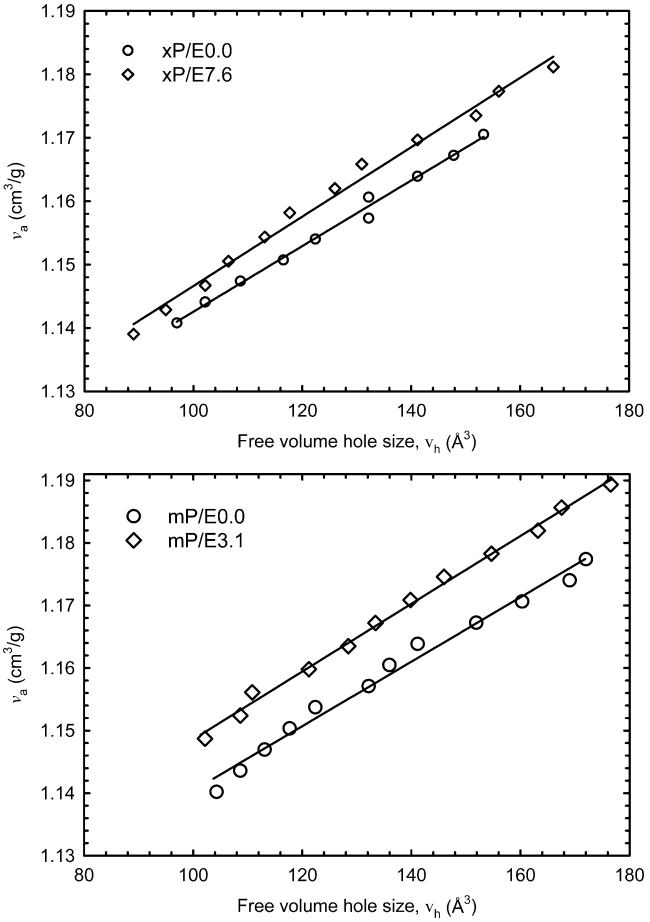

Figure 9. Specific volume of the amorphous phase, v_a, plotted vs the free volume hole size, v_h, to determine N_h' according to eq 5.

Table 3. Results of PALS Studies

material	$T_{g,PALS}$ (°C)	$e_{h,g}$ (Å^3/K)	$e_{h,r}$ (Å^3/K)	v_h[a] (Å^3)	N_h' (10^{20} g^{-1})	v_{occ} (cm^3/g)	N_h[a] (10^{20} cm^{-3})	FFV[a]	*FFV* (at T_g)
xP/E0.0	11	0.19	1.27	101	5.2	1.091	4.5	0.046	0.039
xP/E4.3	6	0.19	1.31	104	5.2	1.095	4.5	0.046	0.037
xP/E7.6	0	0.20	1.39	111	5.5	1.092	4.7	0.053	0.038
xP/E12.1	−5	0.20	1.53	121	5.3	1.093	4.6	0.056	0.037
xP/E16.1	−10	0.21	1.55	129	5.4	1.091	4.7	0.060	0.037
xP/E19.2	−17	0.20	1.49	136	5.9	1.086	5.1	0.069	0.039
mP/E0.0	16	0.22	1.29	97	5.2	1.089	4.5	0.044	0.040
mP/E3.1	16	0.26	1.36	98	5.4	1.094	4.7	0.046	0.042
mP/E11.0	−1	0.24	1.62	122	5.1	1.089	4.4	0.054	0.038
mP/E13.6	−6	0.28	1.45	123	5.7	1.084	4.9	0.060	0.041
mP/E18.8	−11	0.29	1.63	139	5.3	1.087	4.5	0.063	0.039
mP/E25.2	−17	0.25	1.62	141	5.6	1.091	4.8	0.067	0.038

[a] Data for 23 °C.

the literature for a noncrystallizable ethylene/propylene (E/P) copolymer.[28] Literature reports for the specific volume of LLDPE and an isotactic propylene copolymer (i-PP) in the melt follow almost the same curve.[28] This correspondence supports the assumption that the rubbery amorphous density of a noncrystalline P/E copolymer is independent of the ethylene content.

The nonequilibrium glassy line is constructed from v_a of xP/E19.2 at the T_g, which defines the intersection with the equilibrium liquid line. In the absence of bulk thermal expansivity of the amorphous glassy phase, the thermal expansivity is estimated from the hole thermal expansivity in the glass. Assuming that the number of free volume holes in the glass is the same as in the rubbery state, the nonequilibrium thermal expansivity is estimated as 1.1×10^{-4} cm^3 g^{-1} K^{-1} from hole

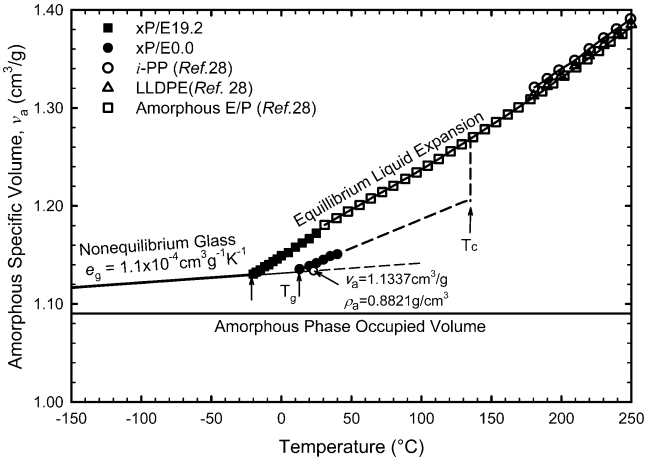

Figure 10. Schematic showing the temperature dependence of the amorphous phase specific volume for P/E copolymers. The data for xP/E0.0 and xP/E19.2 are included as filled symbols. The data taken from ref 28 are shown as open symbols.

density of 5.5×10^{20} g^{-1} and hole thermal expansivity of 0.20 Å^3 K^{-1} in the glass. A single glassy line for all the copolymers seems justified given that free volume hole size in the glass (see Figure 8), hole thermal expansion coefficient in the glass, and the number of free volume holes (see Table 3) are not very sensitive to the amount of crystallinity.

The amorphous phase specific volume for a copolymer with low crystallinity (xP/E19.2, $X_c = 6\%$) is included in Figure 10. The results closely follow the equilibrium curve, as defined by the amorphous P/E, to the glass transition at about −20 °C. The correspondence indicates that the crystallinity of xP/E19.2 is too low to significantly constrain the amorphous phase chains.

Results for a high crystallinity polymer (xP/E0.0, $X_c = 45\%$) are also included. In this case, the amorphous phase specific volume falls well below the equilibrium line. If the copolymer is crystallizable, it follows the equilibrium curve during cooling from the melt until it starts to crystallize at T_c. Once nucleation happens, crystallization typically occurs over a small temperature change and is accompanied by a large decrease in bulk specific volume. Immobilization of chain segments in crystals constrains the attached amorphous chain segments. As a result, the amorphous specific volume also decreases abruptly during crystallization as suggested by the dashed line. The PALS results indicate that the constraint acts primarily to decrease the free volume hole size, rather than to decrease the number of free volume holes. The constrained and densified amorphous phase of xP/E0.0 has a lower thermal expansion coefficient than the equilibrium amorphous polymer (see Table 2), and the amorphous phase contracts along a different liquid line until the line intersects the glass line at a glass transition temperature of about 10 °C. The behavior of the other copolymers lies in between that of xP/E19.2 and that of xP/E0.0. According to Figure 10, the completely constrained amorphous phase would have density 0.882 g cm^{-3}. This is significantly lower than the value of 0.900 g cm^{-3} obtained by extrapolation of ρ_a to 100% crystallinity (see Figure 6). It may be that ρ_a reaches a limit as indicated by the lower dashed line in Figure 6.

According to the concepts of free volume in amorphous polymers,[29,30] the fractional free volume (*FFV*) is constant in the glassy state and increases linearly with temperature above T_g. The *FFV* in the amorphous phase of P/E copolymers was calculated according to refs 13−15

$$FFV = \frac{N_h' v_h}{v_a} \quad (6)$$

and the results are plotted as a function of crystallinity in Figure 11. The large decrease of *FFV* at 23 °C with increasing crystallinity, from 0.068 to 0.039, and the corresponding increase in amorphous phase density are primarily due to the decrease in the hole size (see Figure 8).

To obtain *FFV* at T_g from eq 6, the hole density at T_g was assumed to be equal to N_h', v_h at T_g was taken from the v_h-T plot at $T_{g,PALS}$ (see Figure 7), and v_a was taken from the v_a-T plot, also at $T_{g,PALS}$ (see Figure 5). The *FFV* at T_g was constant across the crystallinity range of the P/E copolymers with a value about 0.04 (Figure 11), in agreement with iso-free volume concepts of the glass transition. In this case, a small decrease in hole density with crystallinity was offset by a small increase in hole size at T_g (see Table 3). However, it should be pointed out that the density of free volume holes changed very little with crystallinity. Thus, the T_g could also be described by an iso-free volume hole size condition within the experimental scatter. It has been pointed out that the iso-free volume condition at T_g may not hold among different polymers, and *FFV* at T_g could be in the range 0.02−0.13.[31] Considering the chemical similarity of the P/E copolymers, the iso-free volume condition at T_g is consistent with this view, and the value of 0.04 is reasonable. Because free volume is closely related to chain dynamics in the amorphous phase, the iso-free volume condition at T_g means that the effect of temperature on amorphous chain mobility is the determining factor, outweighing the effect of constraint imposed by the crystalline phase. Similarity in the thermal expansion coefficient ($e_{h,g}$) of free volume holes in the glassy state (see Figure 7 and Table 3) supports this interpretation.

Conclusions

Recent advances in catalyst technology made it possible to synthesize high molecular weight propylene copolymers with relatively high levels of ethylene comonomer. The availability of copolymers ranging from highly crystalline to almost noncrystalline provided an opportunity to systematically probe the effect of crystallinity on the amorphous phase. The study showed that the rubbery amorphous phase of P/E copolymers ($T > T_g$) densifies with increasing crystallinity, as reflected by higher amorphous phase bulk density (ρ_a) and smaller free volume hole size at ambient temperature. Densification is accompanied by a decrease in the bulk thermal expansivity of the rubbery amorphous phase and a corresponding decrease in the thermal expansivity of free volume holes ($e_{h,r}$). Theses effects reflect reduced mobility of amorphous chain segments as a result of constraint and compaction imposed by connection to chain segments in crystals. The reported discrepancy between the conventional determination of crystallinity from density measured at ambient temperature and crystallinity from heat of melting can now be understood. At least for P/E copolymers, the assumption of constant amorphous phase density is inconsistent with the demonstrated densification of the amorphous phase with increasing crystallinity.

Results from this study, taken together with data from the literature, make it possible to construct the temperature dependence of the amorphous phase specific volume (v_a-T), including the effect of crystallinity. Crystallization modifies the v_a-T relationship by imposing a decrease in amorphous phase specific volume at the crystallization temperature and decreasing the amorphous phase thermal expansion coefficient below the crystallization temperature. As a consequence, the glass transition, defined by the intersection of the thermal expansion lines for rubber and glass, shifts to progressively higher temperatures with increasing crystallinity. Further insight is possible by combining bulk specific volume measurements with free volume hole size from PALS to obtain the fractional free volume (*FFV*). At the glass transition temperature, the *FFV* is constant across the crystallinity range of the P/E copolymers with a value of about 0.04, in agreement with iso-free volume concepts of the glass transition.

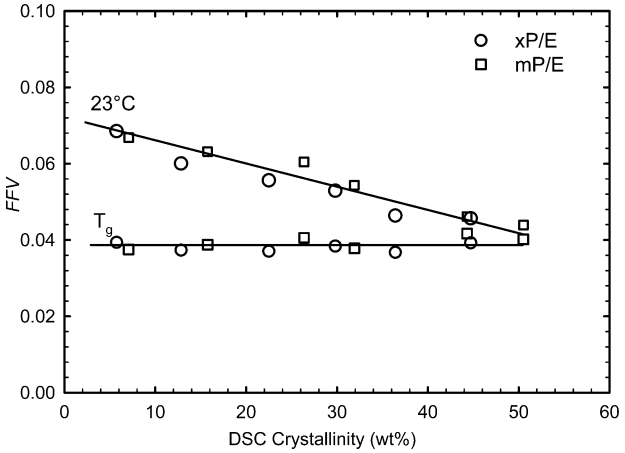

Figure 11. Effect of crystallinity on the fractional free volume (*FFV*) of the amorphous phase at 23 °C and at T_g. The solid lines are to guide the eye.

Acknowledgment. This research was generously supported by The Dow Chemical Co.

References and Notes

(1) Swogger, K. W.; Poon, B.; Stephens, C. H.; Ansems, P.; Chum, S.; Hiltner, A.; Baer, E. In *Proceedings of the Annual Technical Conference of Society of Plastics Engineers*, Nashville, TN, May 4−8, 2003; pp 1768−1774.
(2) Tau, L.-M.; Chum, S.; Karande, S.; Bosnyak, C. U.S. Patent 6,919,-407 B2, 2005.
(3) Bensason, S.; Minick, J.; Moet, A.; Chum, S.; Hiltner, A.; Baer, E. *J. Polym. Sci., Part B: Polym. Phys.* **1996**, *34*, 1301−1315.
(4) Chen, H.; Guest, M. J.; Chum, S.; Hiltner, A.; Baer, E. *J. Appl. Polym. Sci.* **1998**, *70*, 109−119.
(5) Stephens, C. H.; Poon, B. C.; Ansems, P.; Chum, S. P.; Hiltner, A.; Baer, E. *J. Appl. Polym. Sci.*, in press.
(6) Poon, B.; Rogunova, R.; Chum, S. P.; Hiltner, A.; Baer, E. *J. Polym. Sci., Part B: Polym. Phys.* **2004**, *42*, 4357−4370.
(7) Poon, B.; Rogunova, R.; Hiltner, A.; Baer, E.; Chum, S. P.; Galeski, A.; Piorkowska, E. *Macromolecules* **2005**, *38*, 1232−1243.
(8) Isasi, J. R.; Mandelkern, L.; Galante, M. J.; Alamo, R. G. *J. Polym. Sci., Part B: Polym. Phys.* **1999**, *37*, 323−334.
(9) Simha, R.; Somcynsky, T. *Macromolecules* **1969**, *2*, 342−350.
(10) Tao, S. J. *J. Chem. Phys.* **1972**, *56*, 5499−5510.
(11) Nakanishi, N.; Jean, Y. C. In *Positron and Positronium Chemistry*; *Stud. Phys. Theor. Chem. Vol. 57*; Schrader, D. M., Jean, Y. C., Eds.; Elsevier Sci. Publ.: Amsterdam, 1988; pp 159−192.
(12) Pethrick, R. A. *Prog. Polym. Sci.* **1997**, 22, 1−47.
(13) Dlubek, G.; Stejny, J.; Alam, M. A. *Macromolecules* **1998**, *31*, 4574−4850.
(14) Dlubek, G.; Bamford, D.; Rodriguez-Gonzalez, A.; Bornemann, S.; Stejny, J.; Schade, B.; Alam, M. A.; Arnold, M. *J. Polym. Sci., Part B: Polym. Phys.* **2002**, *40*, 434−453.
(15) Srithawatpong, R.; Peng, Z. L.; Olson, B. G.; Jamieson, A. M.; Simha, R.; McGervey, J. D.; Maier, T. R.; Halasa, A. F.; Ishida, H. *J. Polym. Sci., Part B* **1999**, *37*, 2754−2770.
(16) Krigbaum, W. R.; Uematsu, I. *J. Polym. Sci., Polym. Chem. Ed.* **1965**, *3*, 767−776.
(17) Hai-Shan, B.; Cheng, S. Z. D.; Wunderlich, B. *Makromol. Chem., Rapid Commun.* **1988**, *9*, 75−77.

(18) Kluin, J. E.; Yu, Z.; Vleeshouwers, S.; McGervey, J. D.; Jamieson, A. M.; Simha, R.; Sommer, K. *Macromolecules* **1993**, *26*, 1853−1861.
(19) Alamo, R. G.; VanderHart, D. L.; Nyden, M.; Mandelkern, L. *Macromolecules* **2003**, *33*, 6094−6105.
(20) Brandrup, J.; Immergut, E. H. *Polymer Handbook*, 3rd ed.; Wiley: New York, 1989; Section V/27.
(21) Reiger, J. *Polym. Testing* **2001**, *20*, 199−204.
(22) Van Krevelen, D. W. *Properties of Polymers*, 3rd ed.; Elsevier: Amsterdam, 1997; Chapter 7, pp 88−101.
(23) Isasi, J. R.; Alamo, R. G.; Mandelkern, L. *J. Polym. Sci., Part B: Polym. Phys.* **1997**, *35*, 2945−2949.
(24) Kilburn, D.; Bamford, D.; Lüpke, Th.; Dlubek, G.; Menke, T. J.; Alam, M. A. *Polymer* **2002**, *43*, 6973−6983.
(25) Kilburn, D.; Bamford, D.; Dlubek, G.; Piontech, J.; Alam, M. A. *J. Polym. Sci., Part B: Polym. Phys.* **2003**, *41*, 3089−3093.
(26) Schmidt; M.; Maurer, F. H. J. *Macromolecules* **2000**, *33*, 3879−3891.
(27) Bohlen, J.; Kirchheim, R. *Macromolecules* **2001**, *34*, 4210−4215.
(28) Zoller, P.; Walsh, D. J. *Standard Pressure−Volume−Temperature Data for Polymers*; Basel: Technomic, 1995.
(29) Fox, T.; Flory, P. *J. Appl. Phys.* **1950**, *21*, 581−591.
(30) Simha, R.; Boyer, F. *J. Chem. Phys.* **1962**, *37*, 1003−1007.
(31) Yampolskii, Yu. P.; Kamiya, Y.; Alentiev, A. Yu. *J. Appl. Polym. Sci.* **2000**, 76, 1691−1705.

MA0521506